LATERAL-TO-VERTICAL GROWTH TRANSITION OF TiO$_2$ NANORODS GROWN ON FTO-GLASS SUBSTRATE BY HYDROTHERMAL PROCESS

Y. W. LU[a], Y. TSENG[b], J. S. LEE[b], W. J. LEE[b*]

aDepartment of Advanced Thin Films Process, National Pingtung University, Pingtung 90003, Taiwan
bDepartment of Applied Physics, National Pingtung University, Pingtung 90003, Taiwan

In this work, an interesting phenomenon of lateral-to-vertical growth transition occurred in the TiO$_2$ nanorod array (TNA) hydrothermal process is reported. At the initial stage of TNA growth, the TiO$_2$ nanorods (TNs) grew nearly in the lateral direction on the fluorine doped tin oxide coated glass (FTO-glass) substrate. After a period of hydrothermal reaction, the growth direction of TNs was transformed from lateral to vertical direction. In addition, the transition times of lateral-to-vertical growth decreased with increasing hydrothermal temperatures. The transition times of lateral-to-vertical growth are about 4, 3, and 2 h for TNs grown at hydrothermal temperatures of 155, 175, and 195 ^{o}C, respectively. It is suggested that this discovery is useful to help the controlling the TNA morphologies for different applications and the similar phenomenon is probably occurred in growing other materials by hydrothermal process.

1. Introduction

Titanium dioxide (TiO$_2$) is a multi-functional semiconductor of wide bandgap (~3.0 – 3.2 eV). It has been extensively applied to fabrications of electronic and optoelectronic devices such as ultraviolet (UV) photodetectors [1,2], lithium-ion batteries [3,4], dye-sensitized solar cells [5,6], and gas sensors [7,8]. Besides, it has also been used as photocatalysts for pollution decomposition [9,10], anti-bacteria [11,12], and water splitting [13,14].

Recently, TiO$_2$ nanomaterials such as hollow TiO$_2$ nanospheres [15], TiO$_2$ nanowires [16], TiO$_2$ nanotubes [17], and TiO$_2$ nanorods [18], are widely investigated because its nanostructure owns large surface area, which can efficiently improve the device performance. Among these TiO$_2$ nanostructures, the TiO$_2$ nanorod arrays (TNAs) grown by hydrothermal process revealed a single crystal structure in each TiO$_2$ nanorod [19]. This single crystal structure can greatly enhance the device performance due to high carrier mobility and direct pathway for

---

*Corresponding author: wenjenlee@mail.nptu.edu.tw

photogenerated carriers transporting in TiO_2 nanorods (TNs) [20].

The hydrothermal process is a low-cost, vacuum-free, and simple technique for TNA growth on fluorine doped tin oxide (FTO) coated glass substrate that does not need any seed layers due to the same crystalline structure and low lattice-mismatch between TiO_2 and FTO [21,22]. The previous studies reported that TNA grown by hydrothermal process are nearly vertical to the FTO-glass substrate [18,19,23]. However, we found that TNs are not vertically grown in overall hydrothermal process. It is noted that understanding the growing behavior and mechanism of TNs is crucial importance for controlling the different morphologies and microstructures of TNA to meet the requirements of various applications.

In this study, an interesting phenomenon, a lateral-to-vertical growth transition of TNs, occurred in the growing process of TNA grown on FTO-glass substrate by hydrothermal process is discovered. In the initial stage of TNA growth, the TNs exhibit a lateral growing behavior. As the growing process continued, the direction of TNs growth converts to vertical one. Furthermore, the transition times of lateral-to-vertical growth decrease with increasing process temperatures, which are about 4, 3, and 2 h for TNs grown at process temperature of 155, 175, and 195 ^{o}C, respectively.

2. Experimental procedure

In this work, fluorine doped tin oxide (FTO) coated glasses were used as substrates for TiO_2 nanorod array (TNA) grown by hydrothermal process. Before the growth of TNA, the FTO-glass substrates were cleaned by ultrasonic bath in acetone and methanol, followed by rinsing with de-ionized (DI) water and drying in a nitrogen flow. The hydrothermal process of TNA grown on FTO-glass is similar with previous study [24]. A mixture solution contained 30 mL of DI-water, 30 mL of hydrochloric acid (36 wt%, J.T. Baker), and 1 mL of titanium butoxide (97 wt%, Aldrich) was used as precursor for TNA growth. The FTO-glass substrates and precursor solution were placed in a sealed Teflon autoclave, which was then transferred into an electrical oven. The hydrothermal process was carried out in the oven at 155, 175, and 195 ^{o}C for $1 - 9$, $1 - 4$, and $1 - 4$ h, respectively. After the hydrothermal reaction, the autoclave was cooled to room temperature. Finally, the samples were taken out, washed with DI-water and dried in a nitrogen flow for subsequent analysis.

Field-emission scanning electron microscopy (FESEM, Hitachi SU8000) was used for morphological examination of the samples. The growth density, diameter, and thickness of the TNA were analyzed from FESEM images. The crystal structure of the samples was examined by X-ray diffraction (XRD, Rigaku D/MAX2500) with Cu Kα radiation (λ = 1.5406 Å) from 20° to 80° at a scanning speed of 4° min^{-1}.

3. Results and discussion

Figure 1 shows XRD patterns of TNAs grown on FTO-glass substrates. It can be clearly seen that the TNAs grown on FTO-glass substrates at 155 – 195 °C have the same crystalline structure of rutile TiO_2 [see Fig. 1(a)]. According to JCPDS card (No. 88-1175), diffraction peaks at 2θ of 36.4, 41.7, 63.2, 70.1, and 70.4 ° are corresponded to rutile TiO_2 (101), (111), (002) (301) and (112) planes, respectively. Figure 1(b) shows the XRD patterns of TNAs grown on FTO-glass substrate by hydrothermal process at 195 °C for 1 – 4 h. When the hydrothermal reaction time is below 1.5 h, there are no TiO_2 peaks appeared in the XRD patterns and only the diffraction peaks from substrate are detected. From SEM images [Fig. 4(a) and 4(b)], it can be seen obviously that the TNAs appear during the initial growth stage. The TNs are sparsely grown on the FTO surfaces that resulting in the FTO surfaces are not fully covered with TNs. Therefore there are no TiO_2 peaks detected when the hydrothermal reaction time is below 1.5 h since the signal of TNs are not strong enough to meet the detection limit of XRD.
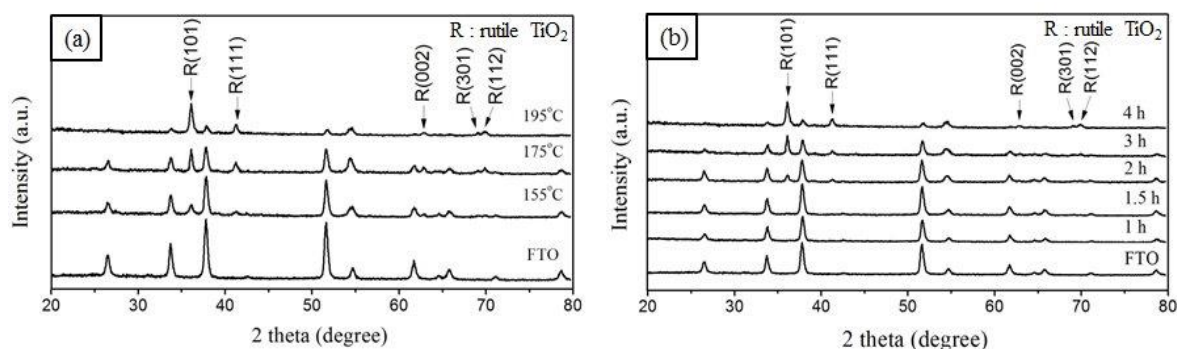
Fig. 1. XRD patterns of TNAs grown on FTO-glass substrates: (a) at indicated temperatures for 4 h, and (b) at 195 °C for 1 – 4 h.

The (101) peak of rutile TiO_2 starts to appear in the XRD pattern after 1.5 h of hydrothermal process. Moreover, the (101) peak gradually increases with increasing hydrothermal reaction time and becomes the strongest peak that can be attributed to the increased thickness of TNA.

Fig. 2 shows the SEM images of TNAs grown on FTO-glass substrates by hydrothermal process at 155 °C with the reaction time varied from 2 to 4 h. It can be clearly seen that the average diameters of TNs and thicknesses of the TNAs increase with increasing reaction time. When the reaction time is 2 h, only textured FTO grains can be observed on the substrate at low magnification. However, it is found that a few tiny TNs start to grow from FTO grain boundaries due to the early nucleation and growth at the grain boundaries [see the insert of Fig. 2(a)]. When the reaction time prolongs to 3 h, these tiny TNs continue to grow laterally from FTO grain

boundaries. Besides, it is noticed that numerous FTO grains remain smooth surfaces where no TNs are found during this initial growth stage. Because the grain boundaries have higher defect densities comparing with the grain faces of FTO, this causes priority nucleation on the grain boundaries.
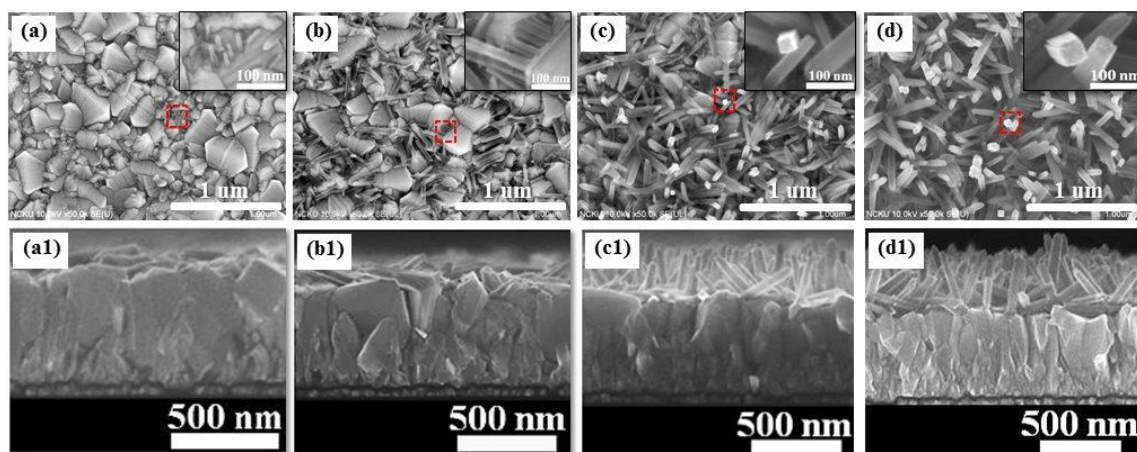
Fig. 2. SEM images of TNAs grown on FTO-glass substrates by hydrothermal process at 155 ^{o}C for (a) 2, (b) 3, (c) 3.5, and (d) 4 h. (a) – (d) show the top-view images (the enlargements of selected area are inserted) and (a1) – (d1) are the corresponding cross-sectional images.

For hydrothermal reaction time between 3 and 3.5 h, an interesting phenomenon of lateral-to-vertical transition of TNs growth is observed. It is noticed that the thickness of TNA is difficult to be identified when the reaction time is below 3.5 h due to the laterally grown TNs and the incompletely covered FTO surface. When the reaction time is increased to 3.5 h, some TNs have transformed to vertical growth on the FTO surface. The cross-sectional image shows the TNs are nearly perpendicular to the FTO surface. After 4 h of growing, the vertical TNs grow densely and uniformly over the entire FTO surface, and the average thickness of TNAs increases from 302 nm to 409 nm with increasing reaction time varied from 3.5 to 4 h. The growth transition of TNs can be described as follows: Because the surface of the FTO has a textural morphology woven by the FTO grains, therefore, the TNs will grow in a fashion with some angles to the FTO surface instead of being perpendicular it. Besides, the density of the grown TNs increases with increasing reaction times at the initial stage of TNA growth. The high TNs density at initial stage is a result of a situation that the space for lateral growth of the germinated TNs is insufficient, thus, only the nearly perpendicular TNs can grow in such condition.

Figure 3 shows the SEM images of TNAs grown on FTO-glass substrate by hydrothermal process at 175 ^{o}C with the reaction time varied from 1 to 4 h. It is clearly observed that the average diameters of TNs and thicknesses of TNAs increase with increasing reaction times. When

the reaction time is 1 h, the FTO surface reveals many FTO grains and the TNs cannot be observed obviously at low magnification. However, it is found that few papilla-like nanoparticles and some tiny TNs begin to grow from grain boundaries on the FTO surface [see insert of Fig. 3(a)]. When the reaction time prolongs to 2 h, the TNs have passed the lateral growth stage and became a vertical one on the FTO surface, suggesting that increasing process temperature not only speeds up the hydrothermal reaction but also shrinks the transition time of the lateral-to-vertical growth. Nevertheless, the cross-sectional image [see Fig. 3(b1)] shows the TNs have a poor growth orientation. When the reaction time increases to 3 h, the TNs are grown densely and almost vertically on the substrate. The result indicates that the growth orientation of TNs can be improved to be vertical by increasing reaction times [see Fig. 3(c1)]. After 4 h, the nearly vertical TNs are grown uniformly on the substrate. The average thicknesses of TNAs are elongated from 210 nm to 918 nm when the reaction time lengthens from 2 to 4 h.
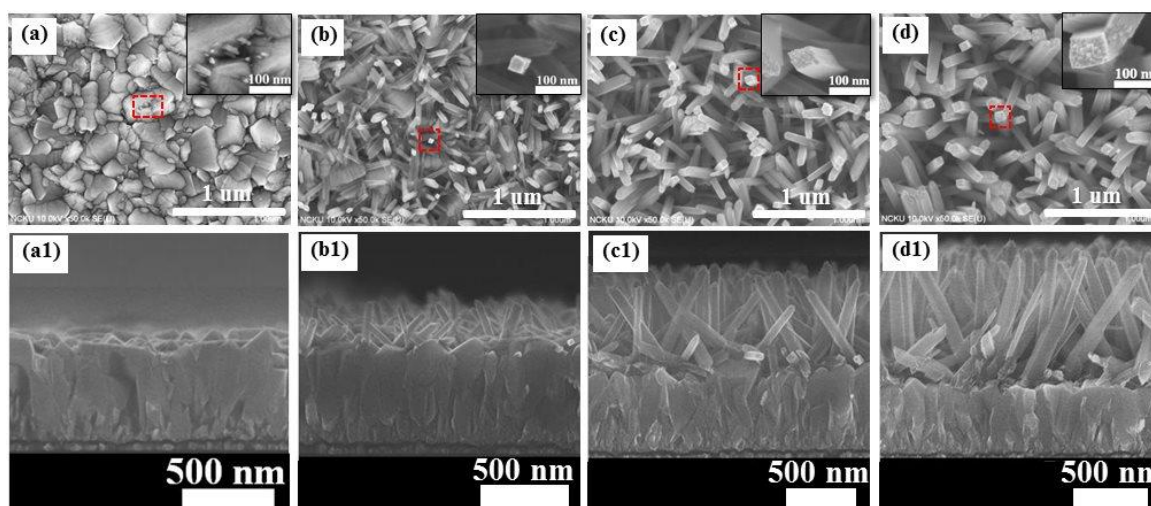
Fig. 3. SEM images of TNAs grown on FTO-glass substrates by hydrothermal process at 175°C for (a) 1, (b) 2, (c) 3, and (d) 4 h. (a) – (d) show the top-view images (the enlargements of selected area are inserted) and (a1) – (d1) are the corresponding cross-sectional images.

Figure 4 shows the SEM images of TNAs grown on FTO-glass substrate by hydrothermal process at 195°C with the reaction time varied from 1 to 3 h. It can be seen that the lateral-to-vertical growth transition of TNs grown at 195 °C appears early at reaction time about 1.5 h comparing to about 3.5 h and 2 h for TNAs grown at 155 and 175 °C. In addition, some TNs are grown at a small angle to the substrate [see Fig. 4(a1)]. For 1.5 h, the cross-sectional image shows that grown TNs are partially lateral and partially vertical on the substrate [see Fig. 4(b1)]. When the reaction time is increased to 3 h, the TNs display a uniform coverage on the FTO surface. In addition, the average thicknesses of TNAs increase from 395 to 1095 nm when the reaction time is changed from 1.5 to 3 h.
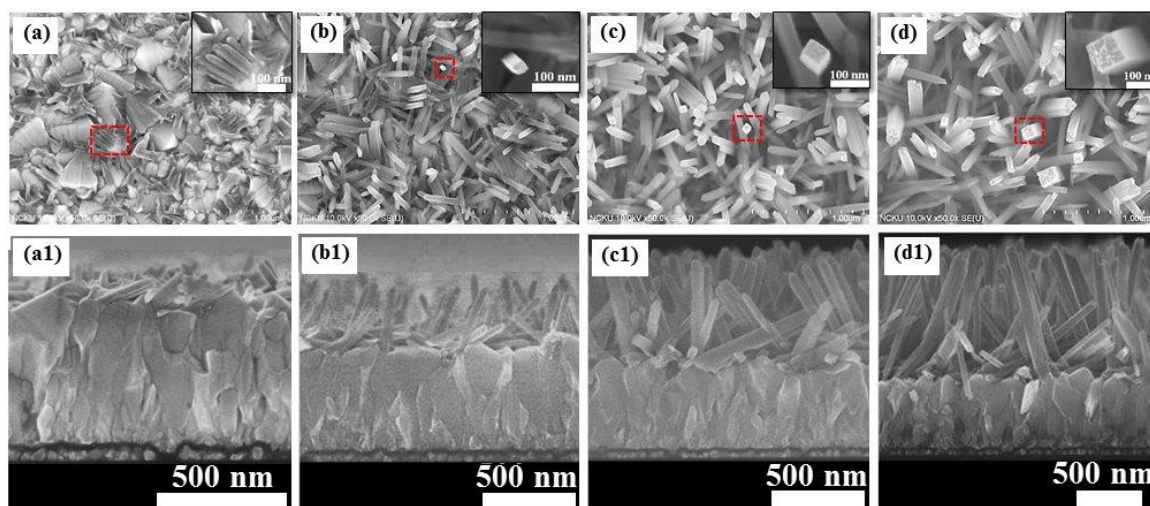
Fig. 4. SEM images of TNAs grown on FTO-glass substrates by hydrothermal process at 195 °C for (a) 1, (b) 1.5, (c) 2, and (d) 3 h. (a) – (d) show the top-view images (the enlargements of selected area are inserted) and (a1) – (d1) are the corresponding cross-sectional images.

The average thicknesses of TNAs measured from cross-sectional SEM images are shown in Fig. 5(a). The average thicknesses of TNAs grown at 155, 175, and 195 °C for 3.5 – 9, 2 – 4, and 1.5 – 4 h are about 302 – 1038, 210 – 918, and 395 – 1566 nm, respectively. The results show that the average thicknesses of TNAs increase with increasing reaction times due to faster reaction-rate for higher reaction temperature.
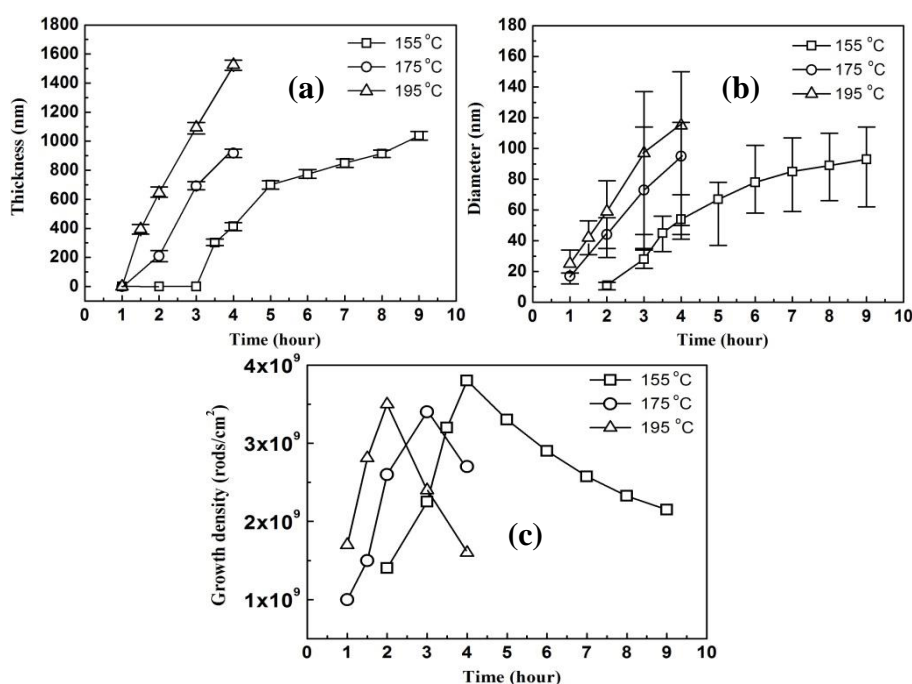
Fig. 5. (a) thickness, (b) diameter, and (c) growth density variations of the TNAs grown on FTO-glass substrates at 155, 175, and 195 °C for the reaction times of 1 – 9, 1 – 4, and 1 – 4 h, respectively.

The average diameters of TNs measured from top-view SEM images are shown in Fig. 5(b). The average diameters of TNs grown at 155 $^{\circ}$C for 2, 3, 3.5, 4, 5, 6, 7, 8, and 9 h are about 11, 28, 45, 54, 67, 78, 85, 89, and 93 nm, respectively. The average diameters of TNs grown at 175 $^{\circ}$C for 1, 2, 3, and 4 h are about 17, 44, 73, and 95 nm, respectively. The average diameters of TNs grown at 195 $^{\circ}$C for 1, 1.5, 2, 3, and 4 h are about 25, 42, 59, 97, and 115 nm, respectively. The results show that the average diameters of TNs increase with increasing reaction times. Furthermore, the diameters range from 41 to 70 nm, 50 to 117 nm, and 44 to 150 nm for the TNs grown at 155, 175, and 195 $^{\circ}$C with hydrothermal reaction times of 4 h, respectively. It can be clearly seen that the TNs grown at 195 $^{\circ}$C have the largest diameter and the broadest distribution in diameter. Because the TNs grown at 195 $^{\circ}$C have the fastest reaction-rate and the early nucleated TNs experienced a longer reaction time than the later nucleated TNs, thus, the TNs grown at 195 $^{\circ}$C have the largest diameter and the broadest diameter distribution. It is also found that the TNs have similar minimum diameters of about 41, 50, and 44 nm for TNs grown at 155, 175, and 195 $^{\circ}$C for 4 h, respectively. Because these are later nucleated TNs, which suffered a shorter reaction time and resulting in a small diameter.

The growth densities of TNs are calculated from top-view SEM images in 2 μm^2 area each. As shown in Fig. 5(c), the growth densities of TNs grown at 155 $^{\circ}$C for 2, 3, 3.5, 4, 5, 6, 7, 8, and 9 h are about 1.4×10^{-9}, 2.25×10^{-9}, 3.2×10^{-9}, 3.8×10^{-9}, 3.3×10^{-9}, 2.9×10^{-9}, 2.6×10^{-9}, 2.3×10^{-9}, and 2.1×10^{-9} rods/cm^2, respectively. The growth densities of TNs grown at 175 $^{\circ}$C for 1, 2, 3, and 4 h are about 1.0×10^{-9}, 2.6×10^{-9}, 3.4×10^{-9}, and 2.7×10^{-9} rods/cm^2, respectively. The growth densities of TNs grown at 195 $^{\circ}$C for 1, 1.5, 2, 3, and 4 h are about 1.7×10^{-9}, 2.8×10^{-9}, 3.5×10^{-9}, 2.4×10^{-9}, and 1.6×10^{-9} rods/cm^2, respectively.

As shown in Fig. 5(c), the TNs grown at 155, 175, and 195 $^{\circ}$C have the same trend in growth density variation that two different stages for growth density variation are found. For the first stage, the growth densities are increased with increasing hydrothermal reaction times. For the second stage, the growth densities will reach the maximum after a period of reaction time and then decrease with prolonged reaction times. Because the TNs have a laterally growing behavior at the initial growth stage and the growth numbers of TNs are direct proportioned to the process temperatures and reaction times that resulted in an existence of the first stage for growth density variation. Following increased reaction times, the grown TNs reached the maximum density. At the same time, the high density limited the lateral growing space of TNs and thus the TNs growing direction changed from lateral to vertical. It can be clearly identified that the maximum densities (the turning points of growth density variation) are 4, 3, and 2 h for TNs grown at 155, 175, and 195 $^{\circ}$C, respectively. These figures correspond to the SEM analyzed results [according to the Fig. 2(d), Fig. 3(c), and Fig. 4(c)], where the lateral-to-vertical growth transition times are 4, 3, and 2 h for TNs grown at 155, 175, and 195 $^{\circ}$C, respectively. For the second stage of growth density variation, the densities decrease with increasing reaction time that is due to the TNs with enlarged dimension reduces the available spaces for TNs growth then causing density decrease.

514

4. Conclusion

The TNAs grown on FTO-glass substrates at 155 – 195 $^{\circ}$C by hydrothermal process are investigated. Furthermore, an interesting phenomenon of lateral-to-vertical growth transition is discovered that the TNs exhibit a lateral growing behavior in the initial growth stage and the growing direction of TNs transformed to vertical one after a period of growth time. Furthermore, the transition times of lateral-to-vertical growth decrease with increasing process temperatures because the growth rate and growth density are directly proportional to the process temperatures. The transition times of lateral-to-vertical growth are about 4, 3, and 2 h for TNs grown at hydrothermal temperatures of 155, 175, and 195 $^{\circ}$C, respectively. In conclusion, the lateral-to-vertical growing behavior of TNs by hydrothermal process has been discovered in this study. It is believed that this discovery can be interested and useful to help the controlling of TNA morphologies for different applications. It is also suggested the similar phenomenon of lateral-to-vertical growth is probably occurred in growing other materials by hydrothermal process.

References

[1] W. J. Lee, M. H. Hon, Appl. Phys. Lett. **99,** 251102 (2011).
[2] A. M. Selman, Z. Hassan, M. Husham, N. M. Ahmed, Appl. Surf. Sci. **305,** 445 (2014).
[3] J. Wang, Y. Bai, M. Wu, J. Yin, W. F. Zhang, J. Power Sources **191,** 614 (2009).
[4] J. S. Chen, Y. L. Tan, C. M. Li, Y. L. Cheah, D. Luan, S. Madhavi, F. Y. Boey, L. A. Archer, X. W. Lou, J. Am. Chem. Soc. **132,** 6124 (2010).
[5] B. O'Regan, M. Grätzel, Nature **353,** 737 (1991).
[6] T. Phonkhokkong, T. Thongtem, S. Thongtem, A. Phuruangrat, W. Promnopas, Dig. J. Nanomater. Bios. **11,** 81 (2016).
[7] C. Garzella, E. Comini, E. Tempesti, C, Frigeri, G. Sberveglieri, Sens. Actuators B **68,** 189(2000).
[8] R. Yordanov, S. Boyadjiev, V. Georgieva, Dig. J. Nanomater. Bios. **9,** 467 (2014).
[9] W. Sangchay, K. Ubonchonlakat, Dig. J. Nanomater. Bios. **10,** 283 (2015).
[10] A. M. Atta, H. A. Al-Lohedan, A. M. Tawfeek, A. A. Abdel-Khalek, Dig. J. Nanomater. Bios. **11,** 91 (2016).

[11] K. Hashimoto, H. Irie, A. Fujishima, Jpn. J. Appl. Phy. **44,** 8269 (2005).

[12] P. Ramesh, S. Muthukkumarasamy, K. Dhanabalan, T. Sadhasivam, K. Gurunathan, Dig. J. Nanomater. Bios. **7,** 1501 (2012).

[13] A. Fujishima, K. Honda, Nature **238,** 37 (1972).

[14] S. U. M. Khan, M. Al-Shahry, W. B. Ingler, Science **297,** 2243 (2002).

[15] W. J. Lee, M. H. Hon, Y. W. Chung, J. H. Lee, Jpn. J. Appl. Phy. **50,** 06GH06 (2011).

[16] X. Feng, K. Shankar, O. K. Varghese, M. Paulose, T. J. Latempa, C. A. Grimes, Nano Lett. **8,** 3781 (2008).

[17] G. K. Mor, K. Shankar, M. Paulose, O. K. Varghese, C. A. Grimes, Nano Lett. **6,** 215 (2006).

[18] J. C. Tsai, M. H. Hon, I. C. Leu, Jpn. J. Appl. Phys. **52,** 06GG09 (2013).

[19] B. Liu, E. S. Aydil, J. Am. Chem. Soc. **131,** 3985 (2009).

[20] K. Yu, J. Chen, Nanoscale Res. Lett. **4,** 1 (2009).

[21] C. J. Howard, T. M. Sabine, F. Dickson, Acta Cryst. **B47,** 462 (1991).

[22] M. Abd-Lefdil, R. Diaz, H. Bihri, M. Ait Aouaj, F. Rueda, Eur. Phys. J. Appl. Phys. **38,** 217 (2007).

[23] Y. Zhao, X. Gu, Y. Qiang, Thin Solid Films **520,** 2814 (2012).

[24] L. G. Teoh, J. S. Lee, Y. Tseng, W. J. Lee, Mater. Trans. **57,** 703 (2016).